ROTATING MOTION CONTROL OF TETHERED SATELLITE CLUSTER SYSTEMS

Osamu MORI
Saburo MATUNAGA

Mechanical and Aerospace Engineering, Tokyo Institute of Technology
2-12-1, O-okayama, Meguro-ku, Tokyo 152-8552, JAPAN
Osamu.Mori@horse.mes.titech.ac.jp

ABSTRACT *– We propose the concept of Tethered Satellite Cluster Systems. The system consists of the satellites connected by tethers, and keeps and changes the formation with active tension/length control of the tether. The purposes of the system are two: the saving of the thruster fuel required for coordinated mission; and the improvement of the control precision, using tether tension. In this paper, we treat the rotating motion; satellites rotate about the center of the mass of the system with the formation in same plane. We establish the coordinated control method using tension and thrust. This control method can decrease the fuel consumption of the thruster, for utilizing tether tension/torque equilibriums. It can also improve the control precision.*

KEYWORDS: Tether, Cluster, Formation Flying, Coordinated Control, Fuel

INTRODUCTION

We propose the concept of Tethered Satellite Cluster Systems[5]. The system consists of satellites connected by tethers and which maintain and change formation using active control of the tension and length of the tether. Such a system can be used in formation flying using the tension of the tether for saving thruster fuel and improving control accuracy as shown in figure 1. The concept can be applied to tethered service satellites[6], which can perform various missions, including autonomic inspection, casting, capture, recovery, moorage, and deorbitting of an uncontrolled satellite.

The features of the tethered satellite cluster systems are the followings.

(1) The system is reconfigurable by tether connection/disconnection between the satellites.

(2) The tether tension and length is controlled by a reel mechanism, and the tether connection/ disconnection is conducted by a joint mechanism.

(3) The reel or joint mechanism is installed on the arms of each satellite.

(4) Each satellite maintains formation flying by coordinated control of position and attitude using the reel, the arm, the thruster and the reaction wheel (RW).

(5) Each satellite can save fuel and improve control accuracy by controlling the tension of the tether.

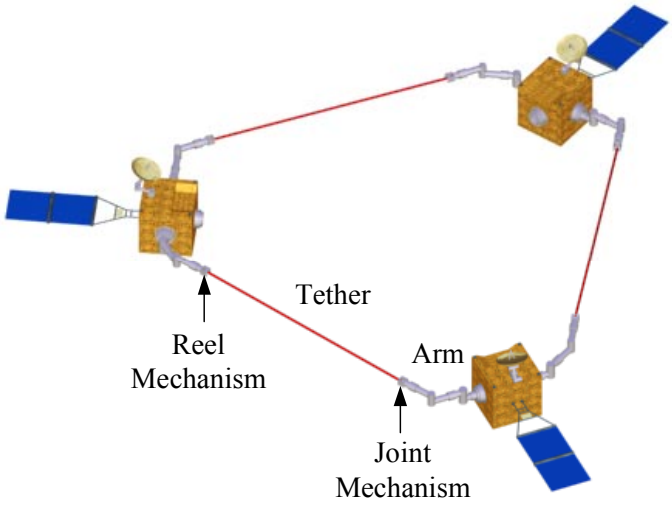

Fig. 1. Tethered Satellite Cluster Systems

In this paper, we consider the rotational motion with respect to the center of the mass (c.m.) of the system in a formation pattern. We treat circular motion as the most fundamental case. We show the equilibrium conditions for maintaining the circular motion using the tether tension, and we establish control methods, based on this equilibrium, for minimizing thruster fuel in this motion. Next, we derive the equilibrium conditions for similar transformation of the system, and we show control methods for saving fuel. Finally, we demonstrate that these control methods are effective in decreasing the position/attitude errors of the satellites as well as reducing the satellite fuel consumption.

MODELING

Figure 2 shows an analytical model of the system. We consider the motions of the n satellites connected by tethers in an earth-centered inertial coordinate system $\{\mathbf{i}\}$. Each satellite, tether and arm is modeled as follows.

Satellite j : The j th satellite ($j = 1, \cdots, n$). The body-fixed coordinate system is $\{\mathbf{b}_j\}$; the mass is m_j; the position of the c.m. is $\mathbf{q}_j$; the moment of inertia about the c.m. is $\mathbf{I}_j$; the angular velocity is $\boldsymbol{\omega}_j$.

Tether jk (Tether kj): Connects satellites j and k . The tension is $T_{jk}\left(=T_{kj}\right)\geq 0$; the mass, twist and bending moment, and tensile strain are ignored.

Arm jk : Deployed on satellite j , and controlling the position $\mathbf{a}_{jk}\left(\neq \mathbf{a}_{kj}\right)$ of the reel or the joint mechanism connected to tether jk .

We define: $\mathbf{F}_j$ and $\boldsymbol{\tau}_j$ are the thrust and the torque vector working on the satellite j as a result of the thruster and the RW; $\mathbf{F}_{jk}$ and $\boldsymbol{\tau}_{jk}$ are the tension and the torque vector due to the tether jk .

ROTATIONAL MOTION

We now consider the rotational motion; n satellites connected to each other by tethers rotate about the c.m. of the system with a target formation on the same plane. We then establish control methods using the tension of the tether.

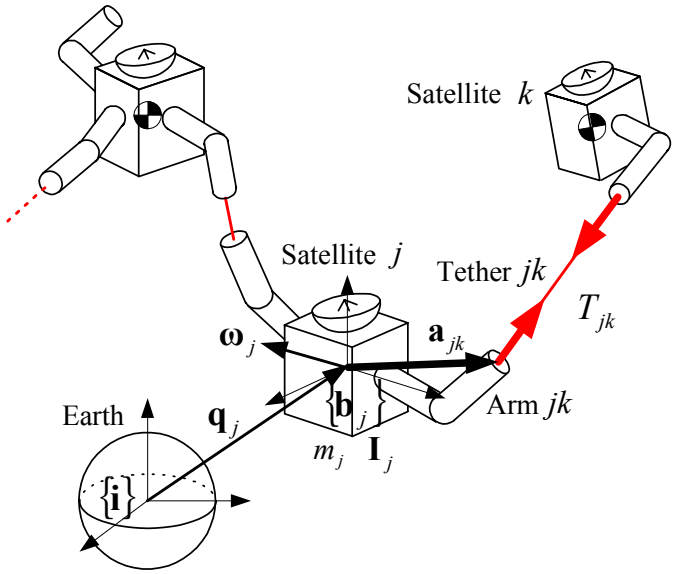

Fig. 2. Analytical Model

Rotational Coordinate System

Figure 3 shows the rotational model in case of $n=3$. The definition of the rotational coordinate system $\{\mathbf{r}\}$ is as follows.

The origin of $\{\mathbf{r}\}$ is the c.m. of the system.

$$\mathbf{q}_{\text{c.m.}} = \sum_{j=1}^{n} m_j \mathbf{q}_j \Big/ \sum_{j=1}^{n} m_j \tag{1}$$

$\mathbf{r}_x\mathbf{r}_y$ represents the rotational plane, and $\mathbf{r}_z$ is the rotational axis. $\mathbf{r}_x$ is the direction of satellite 1 in the rotational plane relative to the c.m. of the system. The relationship between $\{\mathbf{r}\}$ and $\{\mathbf{i}\}$ is defined by the following Euler angles.

$$\{\mathbf{r}\} = C^3(\varphi_r)\{\mathbf{m}\} = C^3(\varphi_r)C^2\left(\theta_r^d\right)C^1\left(\psi_r^d\right)\{\mathbf{i}\} \tag{2}$$

where C is the rotational matrix; $\{\mathbf{m}\}$ is the medium coordinate system; and the superscript d shows the target (set) value. The angular velocity of $\{\mathbf{r}\}$ with respect to $\{\mathbf{i}\}$ or $\{\mathbf{m}\}$ is $\dot{\varphi}_r\mathbf{r}_z$. The angular momentum vector $\mathbf{P}$ of this system is represented as follows.

$$\mathbf{P} = \sum_{j=1}^{n}\left\{m_j\left(\mathbf{q}_j - \mathbf{q}_{\text{c.m.}}\right)\times\left(\dot{\mathbf{q}}_j - \dot{\mathbf{q}}_{\text{c.m.}}\right) + \mathbf{I}_j\cdot\boldsymbol{\omega}_j\right\} \tag{3}$$

The position and attitude of each satellite in $\{\mathbf{r}\}$ is defined as follows.

$$\mathbf{q}_j - \mathbf{q}_{\text{c.m.}} = \{\mathbf{r}\}^T\begin{bmatrix} d_j\cos\lambda_j \\ d_j\sin\lambda_j \\ h_j \end{bmatrix},\ \{\mathbf{b}_j\} = C^1(\psi_j)C^2(\theta_j)C^3(\varphi_j)\{\mathbf{r}\} \tag{4}$$

where, d_j is the distance between the satellite j and the rotational axis; λ_j is the angle between the satellite j and the direction of $\mathbf{r}_x$ in the rotational plane; and h_j is the height of the satellite j out of the rotational plane. In case of a target rotational motion, the direction of $\mathbf{P}$ is equal to that of $\mathbf{r}_z$. And when the rotational angular velocity is relatively large, the gravity term does not change the value of $\mathbf{P}$ because the average of the gravity torque working on the c.m. of the system is zero. In this paper, we assume that the rotational motion satisfies these conditions.

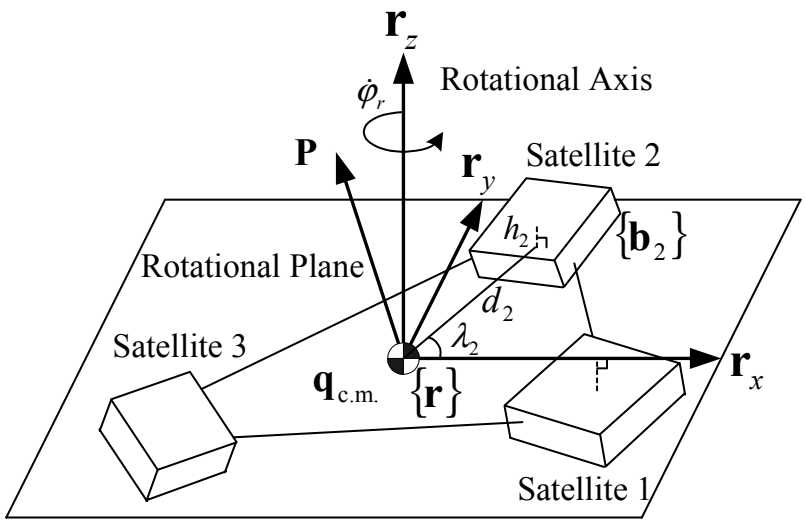

Fig. 3. Rotational Coordinate System

Equilibrium Conditions for Circular Motion

When the system formation in $\{\mathbf{r}\}$ is constant, the rotational motion with respect to $\{\mathbf{m}\}$ is equal to a circular motion. And when the following equilibrium condition is satisfied, the tether tension maintains the motion if gravity terms are ignored. The sum of the tether tension working on each satellite is equal to the centripetal force of the circular motion.

$$\sum_k \mathbf{F}_{jk} = -m_j \dot{\varphi}_r^2 \left(\mathbf{q}_j - \mathbf{q}_{\text{c.m.}}\right) \tag{5}$$

Note that the angular momentum $m_j d_j^2 \dot{\varphi}_r$ of each satellite except for the attitude term is conserved in case of no thruster, because the direction of the sum of tether tension is equal to that of the c.m of the system. We now consider the condition that the tether torque working on the satellite is equal to zero as follows. This is satisfied when the arm direction is equal to the tether direction. The attitude angular momentum $I_j \omega_j$ of each satellite is conserved in case of no RW. Because all satellites are connected to each other, the equilibrium tension for arbitrary formation is represented as follows.

$$T_{jk} = m_j m_k \left|\mathbf{q}_k - \mathbf{q}_j\right| \dot{\varphi}_r^2 / \sum_{l=1}^{n} m_l \tag{6}$$

Coordinated Control Method for Circular Motion

The system uses the reel, the arm, the thruster and the RW for transferring and maintaining the target circular motion. We place importance on saving thruster fuel. We then propose control methods utilizing the tether tension.

Reel/Arm Control

We consider the following feedforward control of the reel and the arm to satisfy the equilibrium conditions.

$$T_{jk} = T_{jk}^d,\ \mathbf{a}_{jk}^d = a_{jk} \frac{\mathbf{q}_k^d - \mathbf{q}_j^d}{\left|\mathbf{q}_k^d - \mathbf{q}_j^d\right|} \tag{7}$$

where T_{jk}^d shows the equilibrium tension for the target circular motion; a_{jk} is the distance between the c.m. of the satellite j and the reel or joint mechanism connected to tether jk.

Thruster/RW Control

We consider the following position/attitude feedback control of the thruster and the RW to transfer to the target circular motion and correct errors.

$$\mathbf{F}_j = -m_j\left\{C_1\left(\dot{\mathbf{q}}_j - \dot{\mathbf{q}}_j^d\right) + K_1\left(\mathbf{q}_j - \mathbf{q}_j^d\right)\right\},\ \boldsymbol{\tau}_j = -\mathbf{I}_j \cdot \left[C_2\left(\boldsymbol{\omega}_j - \dot{\varphi}_r^d \mathbf{r}_z\right) + K_2\left\{\mathbf{b}_j\right\}^T \begin{bmatrix} \psi_j - \psi_j^d \\ \theta_j - \theta_j^d \\ \varphi_j - \varphi_j^d \end{bmatrix} \right] \tag{8}$$

where C and K are the D and P gains, respectively. This control can change the orbital motion, the rotational axis, the rotational angular velocity and the formation in circular motion. By coordination with the reel/arm control, we can save the thruster fuel consumption for maintaining the target motion.

Equilibrium Conditions for Similar Transformation

The similar transformation is defined as an expansion or a reduction of the system formation. Thus the following sum of tether tension maintains the similar transformation of equilibrium formation if gravity terms are ignored.

$$\sum_k \mathbf{F}_{jk} = -m_j\left(\dot{\varphi}_r^2 - \ddot{d}_j / d_j\right)\left(\mathbf{q}_j - \mathbf{q}_{\text{c.m.}}\right) \tag{9}$$

Changing the $\dot{\varphi}_r^2$ term of the equilibrium tension for the circular motion to $\left(\dot{\varphi}_r^2 - \ddot{d}_j / d_j\right)$, we can get the equilibrium tension for similar transformations. Because of $T_{jk} \geq 0$, the relationship $\ddot{d}_j / d_j \leq \dot{\varphi}_r^2$ needs to be satisfied.

Control Method for Similar Transformation

We take advantage of the equilibrium tension for similar transformations. The reel feedforward control inputs the equilibrium tension, and the thruster feedback control causes transfer to the target motion. The arm feedforward control makes the arm direction equal to the tether direction in the target position/ attitude, and the RW feedback control changes the attitude and the angular velocity. The equations for the control method of similar transformations are equal to those for circular motion; equations (7) and (8).

NUMERICAL SIMULATIONS

Considering the rotational motion of three satellites ($n = 3$) connected to each other, we conducted numerical simulations to verify the control methods proposed above.

Simulation Conditions

We set the following parameters for the rotational motion in MKS units.

(1) Satellite Shape

$$m_j = 50\,,\ \mathbf{I}_j = \{\mathbf{b}_j\}^T \begin{bmatrix} 2 & 0 & 0 \\ 0 & 2 & 0 \\ 0 & 0 & 2 \end{bmatrix} \{\mathbf{b}_j\},\ a_{jk} = 1 \tag{10}$$

(2) Initial Conditions

Rotating Coordinate System: $\psi_r^d = \pi/6\,,\ \theta_r^d = \pi/6\,,\ \varphi_r^s = 0\,,\ \dot{\varphi}_r^s = \pi/60$ (11)

Satellite Position: $d_1^s = 20\,,\ d_2^s = 10\,,\ d_3^s = 10\sqrt{3}\,,\ \lambda_2^s = 2\pi/3\,,\ \lambda_3^s = 7\pi/6\,,\ h_j^s = 0$ (12)

Satellite Attitude: $\psi_j^s = 0\,,\ \theta_j^s = 0\,,\ \varphi_j^s = \lambda_j^s + \pi$ (13)

where the superscript s indicates the initial (set) value. All satellites are controlled to be center oriented.

Circular Motion

We consider the case of maintaining the circular motion of the initial conditions by coordinated control of the reel, the arm, the thruster and the RW. Thus the cycle of the circular motion is 120 s.

Figure 4 shows the trajectory of each satellite in the $\mathbf{m}_x\mathbf{m}_y$ plane. The solid, broken and dotted lines in figure 4 represent, respectively, the satellites 1,2 and 3. Figures 5 and 6 show the accumulated thruster impulse and the accumulated RW angular impulse working on satellite 2. The solid, broken and dotted lines represent the three cases of $T_{jk} = T_{jk}^d$, 0 and $1.5T_{jk}^d$. Table 1 shows the average of the position/ attitude errors of satellite 2 for each case.

Figure 4 indicates that the system maintains the target circular motion. The radius of the circular motion of each satellite is d_j^s.

The value in figure 5 is proportional to the fuel consumption of satellite 2. In case of $T_{jk} = T_{jk}^d$, the sum of the tether tension working on the satellite is equal to the centripetal force of the target circular motion. Thus the thruster is used only to correct errors caused by the gravity term, and the accumulated impulse is little. On the other hand, in case of $T_{jk} = 0$ and $1.5T_{jk}^d$ the thruster should supply the centripetal force $m_2 d_2^d \dot{\varphi}_r^{d\,2}$ and the centrifugal force $-0.5 m_2 d_2^d \dot{\varphi}_r^{d\,2}$, respectively. The same is true of the other satellites. Therefore, in the general case of $T_{jk} = \alpha T_{jk}^d$ the accumulated thruster impulse working on satellite j is represented as follows.

$$\int |F_j| dt \approx |1-\alpha| m_j d_j^d \dot{\varphi}_r^{d\,2} t \tag{14}$$

The saving amount of the thruster fuel ($I_{sp} = 75\,\mathrm{s}$) for satellite 2 in case of $\alpha = 1$ is 0.224 kg per circular cycle, compared with in case of $\alpha = 0$. Therefore this control is effective in saving the fuel of the thruster.

The accumulated RW angular impulse is related to the fuel consumption of the thruster because the thruster conducts the RW unloading. Figure 6 indicates that it is nearly equal to zero in all three cases. The reason is that no torque is required for maintaining constant attitude in case of circular motion and that RW is used only to correct attitude errors.

In table 1, the average of the position error is the smallest in case of $T_{jk} = T_{jk}^d$ and it becomes larger in case of $T_{jk} = 1.5T_{jk}^d$ and 0 in that order. And the average of the attitude error is equal to zero in the three

cases. These are the same results as the accumulated thruster impulse and the RW angular impulse. Because of feedback control, the thruster causes the position errors. Therefore suitable feedforward tension is useful in improving the position control accuracy as well as in reducing the fuel consumption of the thruster.

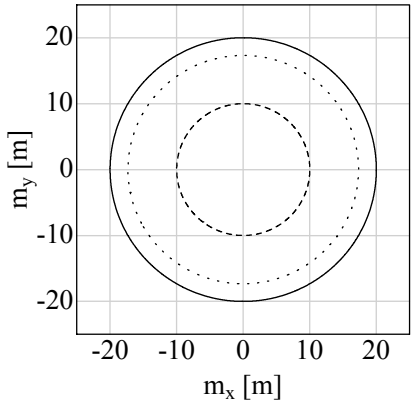

Fig. 4. Trajectory in the $m_x m_y$ Plane (Circular Motion)

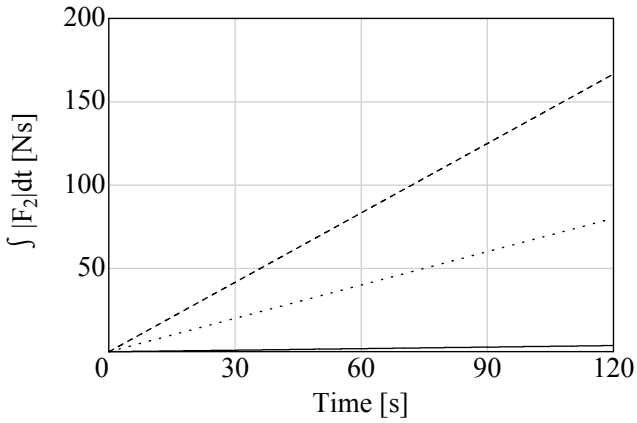

Fig. 5. Accumulated Thruster Impulse of Satellite 2 (Circular Motion)

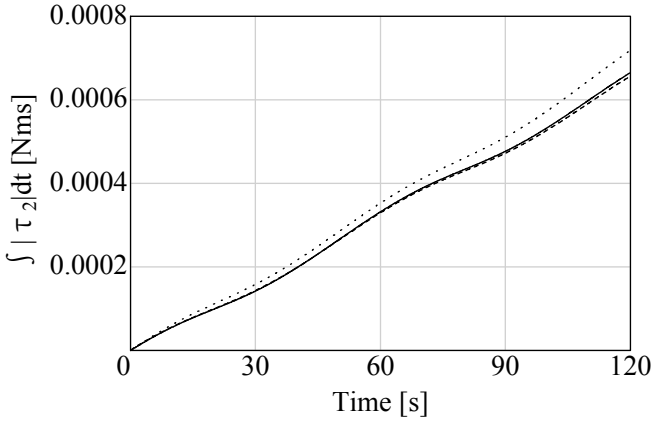

Fig. 6. Accumulated RW Angular Impulse of Satellite 2 (Circular Motion)

Table 1. Average of Position/Attitude Errors of Satellite 2 (Circular Motion)

	$\lvert\Delta q_2\rvert$	$\sqrt{\lvert\Delta\psi_2\rvert^2+\lvert\Delta\theta_2\rvert^2+\lvert\Delta\varphi_2\rvert^2}$
$T_{jk}=T_{jk}^d$	0.000 mm	0.000 deg
$T_{jk}=0$	0.273 mm	0.000 deg
$T_{jk}=1.5T_{jk}^d$	0.137 mm	0.000 deg

Similar Transformation

We consider the following elliptical motion as a similar transformation.

$$d_j^d=\frac{d_{ja}d_{jb}}{\sqrt{d_{ja}^2\cos^2\varphi_r^d+d_{jb}^2\sin^2\varphi_r^d}} \tag{15}$$

where d_{ja} and d_{jb} are the lengths of the major and minor axes of the ellipse. We set $d_{ja}=d_j^s$, $d_{jb}=0.5d_j^s$. Thus the cycle of the elliptical motion is 60 s.

Figure 7 shows the transformation sequence of the motion in the $\mathbf{r}_x\mathbf{r}_y$ plane. Figure 8 shows the trajectory of each satellite in the $\mathbf{m}_x\mathbf{m}_y$ plane. The solid, broken and dotted lines in figure 8 represent, respectively, the satellites 1,2 and 3. Figures 9 and 10 show the accumulated thruster impulse and the accumulated RW angular impulse working on satellite 2. The solid, broken and dotted lines represent the cases for $T_{jk}=T_{jk}^d$, 0 and $1.5T_{jk}^d$. Table 2 shows the average of the position/attitude errors of satellite 2 for each case.

Figures 7 and 8 show that the system achieves the target elliptical motion by similar transformation.

In figure 9, the sum of the tether tension in case of $T_{jk}=T_{jk}^d$ is equal to the centripetal force of the target elliptical motion, and the accumulated thruster impulse is small. The larger the difference between T_{jk} and T_{jk}^d becomes, the larger the accumulated thruster impulse becomes. In general, the accumulated of the thruster impulse in case of $T_{jk}=\alpha T_{jk}^d$ is shown as follows.

$$\int\lvert F_j\rvert dt\approx\lvert 1-\alpha\rvert\int m_j d_j^d\left(\dot{\varphi}_r^{d\,2}-\ddot{d}_j^d/d_j^d\right)dt \tag{16}$$

The graph inclination in figure 9 shows that the centripetal force of the elliptical motion changes cyclically.

The larger the tension becomes, the smaller the accumulated RW angular impulse becomes in figure 10. In a similar transformation, the target angular velocity $\dot{\varphi}_r^d$ changes. Therefore a torque $I_j^d\ddot{\varphi}_r^d$ is necessary for attitude control of the satellite center orientation. In case of $T_{jk}=0$, the accumulated RW angular impulse is nearly equal to $\int\left|I_j^d\ddot{\varphi}_r^d\right|dt$. On the other hand, in case of $T_{jk}\neq 0$, each tether gives the satellites the torque to correct all attitude errors except for the twist. Because the torque is proportional to the tension, accumulated RW angular momentum becomes smaller with increase of the tension.

Figures 9, 10 and Table 2 indicate that the position and attitude errors become smaller with decrease of the thruster impulse and the RW angular impulse. Substituting tether tension/torque for the thruster and the RW, we can save thruster fuel and improve the position and attitude control accuracy. Note that the

smallest case of thruster impulse is different from the smallest case of RW angular impulse; $T_{jk} = T_{jk}^{d}$ and $T_{jk} = T_{\max}$ (maximum tension).

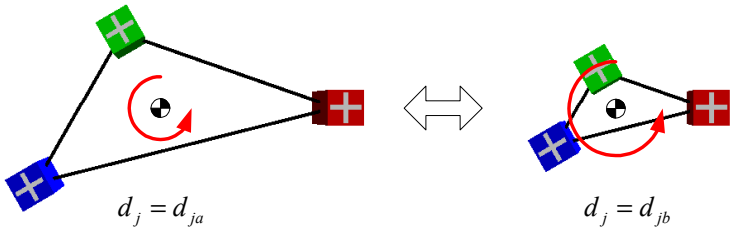

Fig. 7. Motion Sequence in the $\mathbf{r}_x\mathbf{r}_y$ Plane (Similar Transformation)

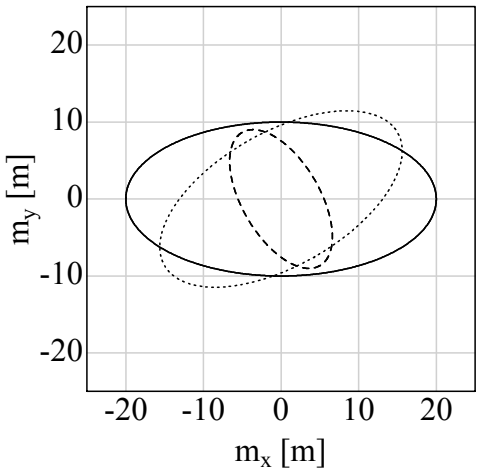

Fig. 8. Trajectory in the $\mathbf{m}_x\mathbf{m}_y$ Plane (Similar Transformation)

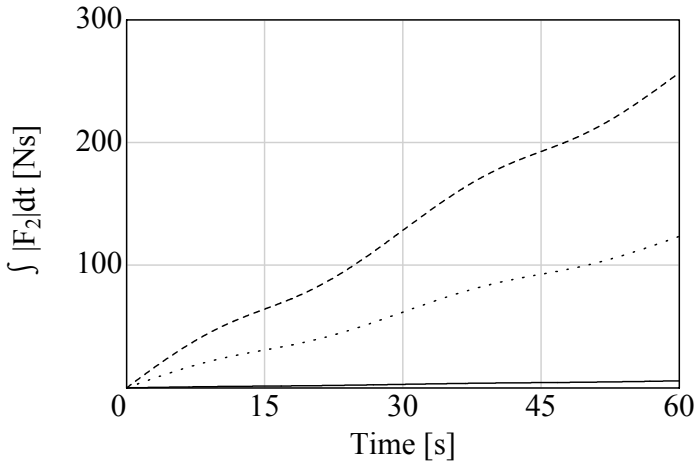

Fig. 9. Accumulated Thruster Impulse of Satellite 2 (Similar Transformation)

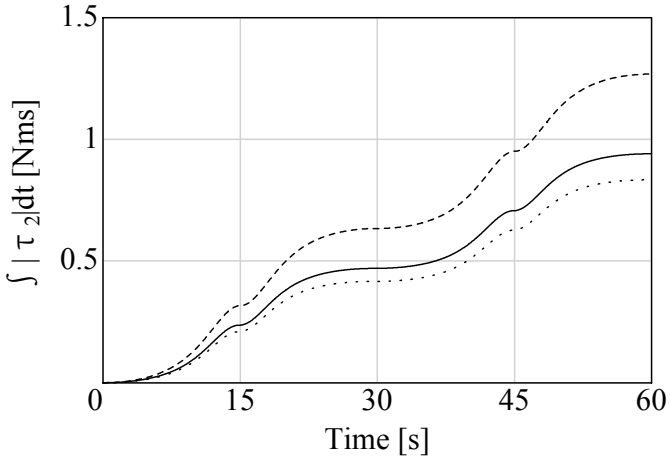

Fig. 10. Accumulated RW Angular Impulse of Satellite 2 (Similar Transformation)

Table 1. Average of Position/Attitude Errors of Satellite 2 (Similar Transformation)

	$\lvert\Delta q_2\rvert$	$\sqrt{\lvert\Delta\psi_2\rvert^2+\lvert\Delta\theta_2\rvert^2+\lvert\Delta\varphi_2\rvert^2}$
$T_{jk}=T_{jk}^d$	0.000 mm	0.049 deg
$T_{jk}=0$	0.843 mm	0.066 deg
$T_{jk}=1.5T_{jk}^d$	0.420 mm	0.043 deg

GROUND EXPERIMENT SYSTEM

We show the concept of two-dimensional ground experiment system as shown in figure 11. This system consists of satellites and ground station as shown in figure 12. The outline is as follows.

Satellite

Each satellite is the rectangular solid ($0.6\,\mathrm{m}\times0.6\,\mathrm{m}\times0.7\,\mathrm{m}$, $m_j=58\,\mathrm{kg}$, $I_j=3.73\,\mathrm{kgm}^2$), floating on the flat floor ($3\,\mathrm{m}\times5\,\mathrm{m}$) with four air pads. It obtains the driving force/torque with eight thrusters. The force and torque of a thruster ($I_{sp}=24.1\,\mathrm{s}$) is 2.22 N and 0.444 Nm. The fuel for thruster or air pad is supplied by tank. The gyro acquires the attitude data of the satellite and the PC communicates with the ground station by wireless LAN (TCP/IP protocol).

Ground Station

The CCD camera gains the pictures of the whole flat floor and the PC calculates the position of satellites by pattern matching. The PC also controls the position/attitude of each satellite through the wireless network.

GROUND EXPERIMENTS

We conduct two rotational experiments of tethered satellite cluster systems; three-satellite circular motion experiment and two-satellite similar transformation experiment.

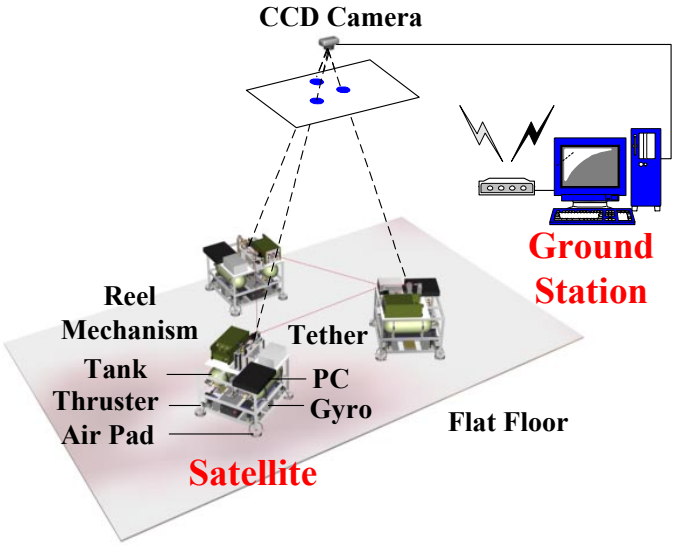

Fig. 11. Two-dimensional Ground Experiment System

Fig. 12. Satellite and Ground Station

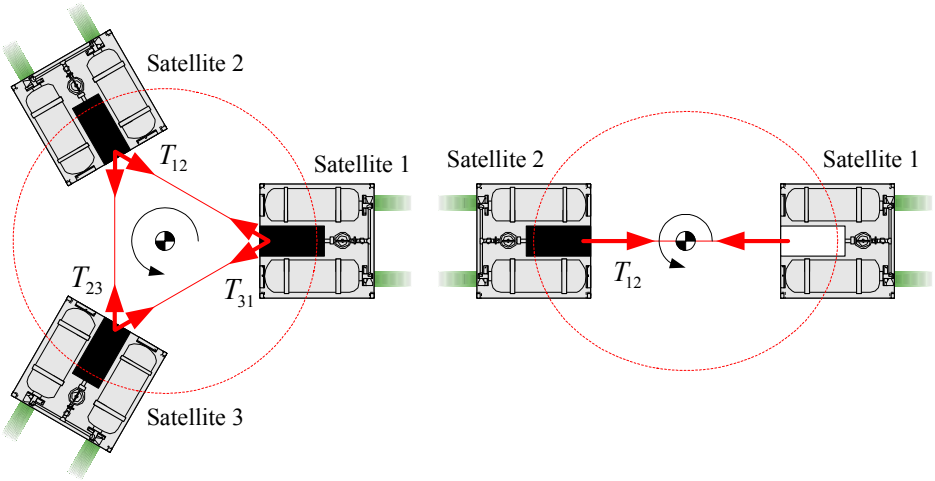

Fig. 13. Experiment Conditions

Experiment Conditions

Figure 13 shows the experiment conditions. The system rotates about the c.m of the system, and the target formations are a regular triangle (three-satellite experiment) and a line (two-satellite experiment). In these experiments the tether connection point of each satellite is fixed ($a_j = 0.26\,\mathrm{m}$). In the target formation/ attitude, the connection point is controlled to be oriented the c.m. of the system. The initial conditions satisfy the target formation/attitude, and we set $d_j^s = 0.8\,\mathrm{m}$ and $\dot{\varphi}_r^s = 2\pi / 30\,\mathrm{rad/s}$.

Three-Satellite Circular Motion

We maintain the circular motion of the initial conditions by coordinated control of the reel and the thruster. The cycle of the circular motion is 30 s, and the equilibrium tension T_{jk}^d of each tether is 1.18 N.

Figures 14 and 15 show the accumulated thruster impulse and the accumulated thruster angular impulse working on satellite 1. The solid, broken, dotted and dashed lines represent the four cases of $T_{jk} = T_{jk}^d$, 0 , $1.5T_{jk}^d$ and $2T_{jk}^d$, respectively. The bold broken lines represent the following theoretical values in case of no tether.

$$\int |F_1| dt = m_1 d_1^d \dot{\varphi}_r^{d\,2} t \ , \ \int |\tau_1| dt = \int \left| I_j^d \ddot{\varphi}_r^d \right| dt \tag{17}$$

Table 3 shows the average of the position/attitude errors of satellite 1 for each case. The results of another satellite are nearly equal to those of satellite 1.

In case of $T_{jk} = T_{jk}^d$ the accumulated thruster impulse is the smallest, however, not equal to zero, because of the friction and inclination of the flat floor, tension error, and pattern matching error. The accumulated impulse in case of $T_{jk} = 0$ is slightly smaller than the theoretical value as shown in equation (17). It also is nearly equal to in case of $T_{jk} = 2T_{jk}^d$. Note that thrust directions in cases of $T_{jk} = 0$ and $2T_{jk}^d$ are opposite each other. The accumulated impulse in case of $T_{jk} = 1.5T_{jk}^d$ becomes the average value of the impulses in cases of $T_{jk} = T_{jk}^d$ and 0 (or $2T_{jk}^d$). The fuel mass difference between two cases of $T_{jk} = T_{jk}^d$ and 0 is 0.0726 kg per circular cycle. These results show tether tension saves the thruster fuel in case of $T_{jk} = T_{jk}^d$. On the other hand, the maximum circular angular velocity in case of $T_{jk} = 0$ is 17.7 deg/s because of the magnitude of thruster force. The tether tension also increases the value in case of $T_{jk} = T_{jk}^d$.

None of the accumulated thruster angular impulses in cases of $T_{jk} = T_{jk}^d$, 0 , $1.5T_{jk}^d$ and $2T_{jk}^d$ is equal to zero, because of the friction and inclination of the flat floor, the ununiformity of thrusters or air pads, and the difference between the center and the c.m. of each satellite. The larger the tension becomes, the smaller the accumulated angular impulse becomes. This is because the tether torque to correct attitude error is proportional to the tension.

The average of position error is the smallest in case of $T_{jk} = T_{jk}^d$, and the average of attitude error is the largest in case of $T_{jk} = 0$ in table 3. If the position/attitude errors are enough small, the direction of the sum of tether tension is equal to the direction of the c.m. of the system. In this case the position error becomes larger with increase of $\left| T_{jk} - T_{jk}^d \right|$, and the attitude error becomes smaller with increase of T_{jk} . In this experiment, however, the position/attitude errors are not ignored, and the relationship is not satisfied.

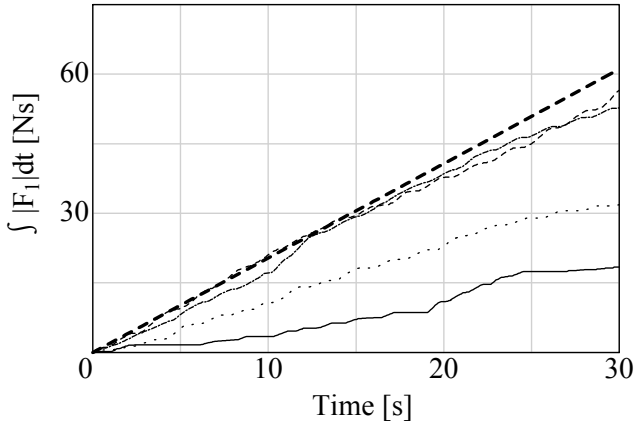

Fig. 14. Accumulated Thruster Impulse of Satellite 1 (Three-Satellite Circular Motion)

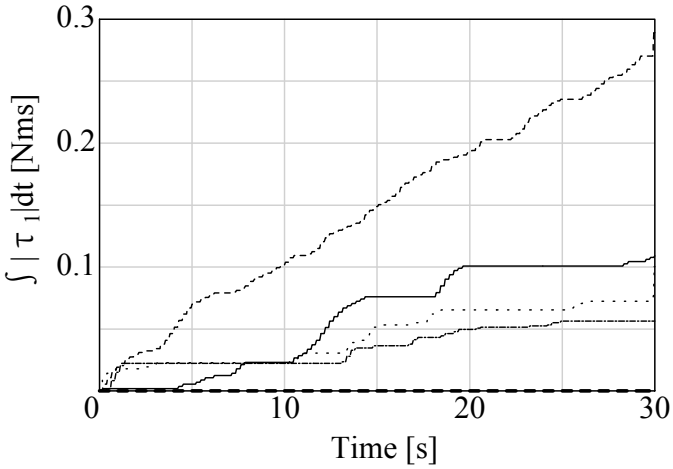

Fig. 15. Accumulated Thruster Angular Impulse of Satellite 1 (Three-Satellite Circular Motion)

Table 3. Average of Position/Attitude Errors of Satellite 1 (Three-Satellite Circular Motion)

	$\lvert\Delta q_1\rvert$	$\lvert\Delta\varphi_1\rvert$
$T_{jk} = T_{jk}^d$	24.7 mm	4.36 deg
$T_{jk} = 0$	31.3 mm	7.00 deg
$T_{jk} = 1.5T_{jk}^d$	34.1 mm	3.61 deg
$T_{jk} = 2T_{jk}^d$	45.7 mm	4.83 deg

Two-Satellite Similar Transformation

As a similar transformation, we conduct the elliptical motion defined in equation (15). We set $d_{ja} = d_j^s$, $d_{jb} = 0.85d_j^s$. The cycle of the elliptical motion is 25.5 s.

Figures 16 and 17 show the accumulated thruster impulse and the accumulated thruster angular impulse working on satellite 1. The solid, broken and dotted lines represent the four cases of $T_{jk} = T_{jk}^d$, 0 and $1.5T_{jk}^d$. The bold broken lines represent the following theoretical values in case of no tether.

$$\int |F_1| dt = \int m_1 d_1^d \left(\dot{\varphi}_r^{d\,2} - \ddot{d}_1^d / d_1^d \right) dt \,,\ \int |\tau_1| dt = \int \left| I_1^d \ddot{\varphi}_r^d \right| dt \tag{18}$$

Table 4 shows the average of the position/attitude errors of satellite 1 for each case.

In case of $T_{jk} = T_{jk}^d$ the accumulated thruster impulse is the smallest, however, not equal to zero, because of the same errors as shown in the accumulated impulse of the three-satellite circular motion. The accumulated impulses in cases of $T_{jk} = 0$ and $1.5T_{jk}^d$ are nearly equal to the theoretical value, and the average of cases of $T_{jk} = T_{jk}^d$ and 0, respectively.

The accumulated thruster angular impulse in case of $T_{jk} = 0$ is smaller than the theoretical value because the errors, mentioned in the accumulated angular impulse of the circular experiment, causes the torque. The larger the tension becomes, the smaller the accumulated angular impulse becomes.

The average of position error is the smallest in case of $T_{jk} = T_{jk}^d$, and the average of attitude error is the largest in case of $T_{jk} = 0$ in table 4. The position and attitude errors in this experiment interfere with each other, because they are not relatively small.

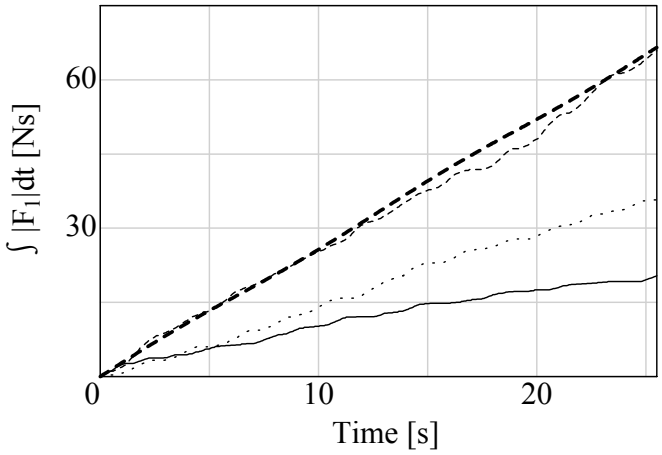

Fig. 16. Accumulated Thruster Impulse of Satellite 1 (Two-Satellite Similar Transformation)

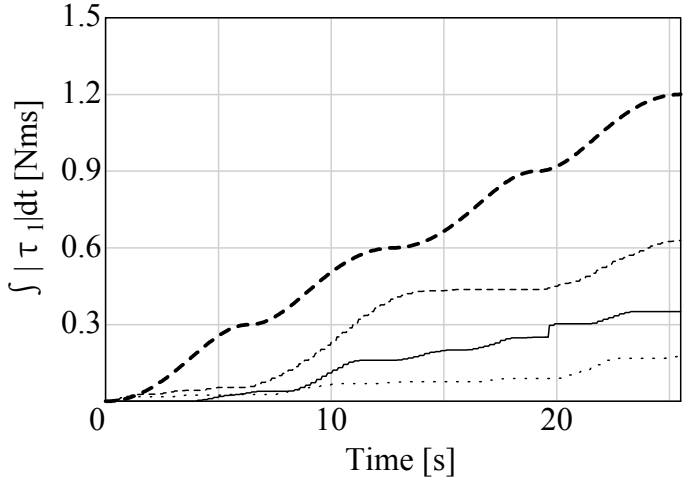

Fig. 17. Accumulated Thruster Angular Impulse of Satellite 1 (Two-Satellite Similar Transformation)

Table 4. Average of Position/Attitude Errors of Satellite 1 (Two-Satellite Similar Transformation)

	$\lvert\Delta q_1\rvert$	$\lvert\Delta \varphi_1\rvert$
$T_{jk} = T_{jk}^d$	21.2 mm	3.31 deg
$T_{jk} = 0$	33.0 mm	9.20 deg
$T_{jk} = 1.5T_{jk}^d$	37.3 mm	3.36 deg

CONCLUSION

In this paper, which represents foundation research of tethered satellite cluster systems, we considered the control for a same-plane formation rotating with respect to the c.m. of the system. We established the following:

(1) We derived the equilibrium conditions for maintaining the system formation and performing circular motion by tether tension. And we proposed a coordinated control method for the circular motion using the reel, the arm, the thruster, and the RW in order to minimize thruster fuel.

(2) We showed the equilibrium conditions when the tether tension changes the system formation similarly. And we established a coordinated control method for the similar transformation.

(3) By numerical simulations and ground experiments, we showed that these control methods can save thruster fuel and improve control accuracy of the position/attitude of each satellite, using the tether tension/torque instead of the thruster/RW.

REFERENCES

[1] R. Cobb, A. Das, K. Denoyer, “TechSat21: Developing Low-Cost, Highly Functional Micro-Satellite Clusters for 21st Centur Air Force Missions,” *50th Congress of the International Astronautical Federation*, 1999.

[2] S. Matunaga, O. Mori, T. Kanzawa, S. Tsurumi and N. Maeda, ”Concept of Robot Satellite Cluster and Ground Experiment System,” *Proceedings of TITech COE/Super Mechano-Systems Workshop*, pp.103-111, 2000.

[3] R. W. Beard, F. Y. Hadaegh, ”Finite Thrust Control for Satellite Formation Flying with State Constraints,” *American Control Conference*, pp.2975-2979, 1999.

[4] S. G. Tragesser, “Formation Flying with Tethered Spacecraft,” *AIAA/AAS Astrodynamics Specialist Conference*, AIAA2000-4133, 2000.

[5] O. Mori, S. Matunaga, “Research and Development of Tethered Satellite Cluster Systems,” *Proceedings of 2000 IEEE/RSJ International Conference on Intelligent Robots and Systems*, Vol.3, pp.1834-1840, 2000.

[6] S. Matunaga, Y. Ohkami and O. Mori, “Tether-Based Capture of Orbiting Objects,” *48th Congress of the International Astronautical Federation*, IAF-97-A.3.08, 1997.